JOURNAL OF AGRICULTURAL AND FOOD CHEMISTRY

pubs.acs.org/JAFC Article

High-Performance Production of *N*-Acetyl-D-Neuraminic Acid with Whole Cells of Fast-Growing *Vibrio natriegens* via a Thermal Strategy

Yuan Peng, Lina Ma, Ping Xu,* and Fei Tao*

Cite This: https://doi.org/10.1021/acs.jafc.3c07259 Read Online

ACCESS | Metrics & More | Article Recommendations | Supporting Information

ABSTRACT: High performance is the core objective that biotechnologists pursue, of which low efficiency, low titer, and side products are the chief obstacles. Here, a thermal strategy is proposed for simultaneously addressing the obstacles of whole-cell catalysis that is widely applied in the food industry. The strategy, by combining fast-growing *Vibrio natriegens*, thermophilic enzymes, and high-temperature whole-cell catalysis, was successfully applied for the high-performance production of *N*-acetyl-D-neuraminic acid (Neu5Ac) that plays essential roles in the fields of food (infant formulas), healthcare, and medicine. By using this strategy, we realized the highest Neu5Ac titer and productivity of 126.1 g/L and up to 71.6 g/(L h), respectively, 7.2-fold higher than the productivity of *Escherichia coli*. The major byproduct acetic acid was also eliminated via quenching complex metabolic side reactions enabled by temperature elevation. This study offers a broadly applicable strategy for producing chemicals relevant to the food industry, providing insights for its future development.

KEYWORDS: *N-acetylneuraminic acid, thermophilic enzyme, Vibrio natriegens, whole-cell catalysis, rapid biotechnology, metabolic chaos*

Downloaded via SHANGHAI JIAO TONG UNIV on December 9, 2023 at 09:03:34 (UTC).
See https://pubs.acs.org/sharingguidelines for options on how to legitimately share published articles.

INTRODUCTION

Advances in synthetic biology have brought the eruption of biotechnology, gradually reshaping the traditional production modes.[1,2] Specifically, it has facilitated the advancement of the food industry by providing varied novel technologies, such as whole-cell catalysis. However, low efficiency remains ubiquitous in bioproduction systems. Developing high-performance production with biotechnology is also hindered by the chaotic nature of cellular metabolism, which consists of thousands of enzymes, metabolites, and their interactions, posing significant challenges to achieving high titer, productivity, and purity.[3] Traditional solutions rely mainly on genetic manipulations including gene-knockout and gene-knockdown with genetic tools such as homologous recombination and CRISPR-Cas-mediated gene editing.[4,5] However, dozens of genes usually need to be simultaneously targeted, and uncharacterized reactions often exist, thus additionally increasing the execution difficulties.[6] Developing an efficient technology is often time consuming and labor intensive. Therefore, establishing a method that can improve production efficiency and control metabolic chaos in a versatile manner is urgently demanded.

It is worth noting that chemical production usually tends to have higher reaction rates compared to bioproduction, which is mainly contributed by the utilization of higher temperatures.[7] Elevating temperature of enzymatic catalysis has been applied in food, paper, and textile processing, due to the advantages such as high reaction rates, robustness, and compatibility to processing operations.[8,9] For example, thermophilic amylases are used to accelerate the starch liquefaction process.[10,11] Thermophilic enzymes, such as pullulanases, cyclodextrin, glycosyltransferases, and cellulases, show unique advantages in the food, chemical, pharmaceutical industries, and environmental biotechnology.[12] Consequently, high-temperature production with thermophilic enzymes presents a highly favorable prospect for future biotechnology.

Vibrio natriegens is the fastest-growing Gram-negative marine bacterium.[13−15] Its high substrate uptake rates, fast protein expression rates, and metabolic prowess make it a promising next-generation workhorse for rapid biotechnology and it has been increasingly attractive to biotechnologists.[15−17] At present, extensive research is focused on the development of genetic tools for *V. natriegens* to develop an emerging next-generation chassis.[16−18] Some valuable chemicals such as alanine, 2,3-butanediol, and 1,3-propanediol have been successfully synthesized with *V. natriegens*.[18−20] As a potentially excellent protein expression chassis, *V. natriegens* allows protein expression to be both fast and preferably soluble.[16,21] Additionally, *V. natriegens* is nonpathogenic, and there are no health hazards when applied in food biotechnology. Therefore, *V. natriegens* is increasingly accepted as a superior chassis that can significantly promote the efficiency of biotechnology.

Side reactions are often inevitable in the process of bioproduction partly because of the chaos of metabolism.[22−24] Specifically, when the reaction temperature is close to the optimal growth temperature of the chassis, the enzymes involved in cellular central metabolism are active, which exist simultaneously with the desired pathways.[25] They will decrease the purity of the target, increase challenges in the product purification, and typically necessitate laborious and time-

Received: October 7, 2023
Revised: November 22, 2023
Accepted: November 23, 2023

ACS Publications © XXXX American Chemical Society

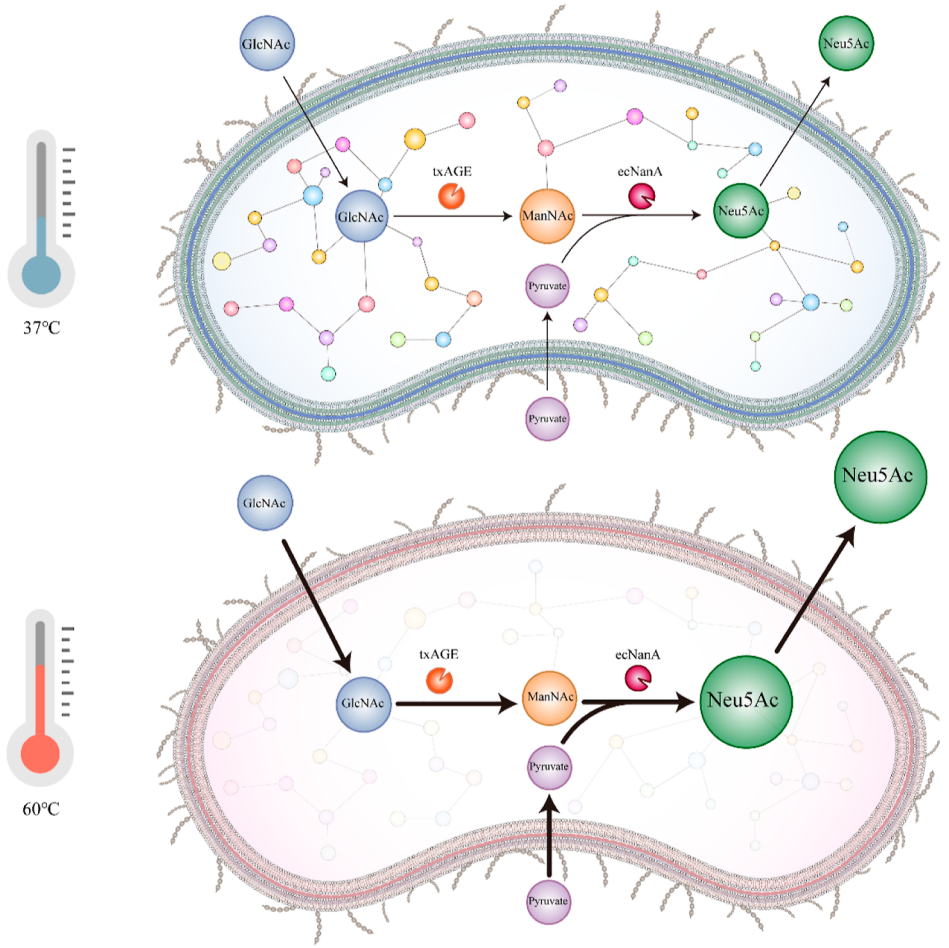

Figure 1. Scheme of the thermal strategy for high-performance Neu5Ac production. Low efficiency, low titer and side products are fundamental obstacles of high-performance whole-cell catalysis systems. To solve these problems, we proposed a thermal strategy combining *V. natriegens*, thermophilic enzymes, and high-temperature whole-cell catalysis. Neu5Ac production successfully leaped with this powerful strategy. Usually, the whole-cell catalysis for Neu5Ac production is carried out at mesophilic temperatures such as 37 °C, which is close to the optimal growth temperature of a mesophilic chassis. So, the chaos of cellular metabolism exists, in which endogenetic enzymes inevitably compete with the desired pathways, hindering the target reaction (the upper panel). After using the thermal strategy at 60 °C, high titer and productivity were simultaneously achieved, represented by the ball size and arrow breadth, respectively. As the temperature increased, cellular metabolism's complexity encoded by endogenetic enzymes was significantly reduced, and the corresponding byproduct was significantly eliminated (the lower panel).

consuming genetic manipulations for resolution.[25] Simultaneously, they also compete with desired pathways and result in the degradation of target products.[26] Notably, cellular enzymes in mesophilic chassis can be easily inactivated at elevated temperatures.[27] So, production at high temperatures can also be expected to be capable of inactivating the endogenous enzymes of the mesophilic chassis and reducing the production of byproducts.

N-acetyl-D-neuraminic acid (Neu5Ac) is the primary type of sialic acid in biological systems,[28] which is of tremendous value due to its vital roles in diverse cellular processes. Neu5Ac is defined as the inhibitor of influenza virus A and B infections, and some Neu5Ac derivatives are used for cancer targeting and therapy.[29,30] It also contributes to developing the brain and strengthening the immunity of infants.[31] At present, Neu5Ac has been widely used as an active ingredient in infant formula. Neu5Ac can also be an additive in various dairy products, such as chocolate, milk-based energy drinks, whey protein powder, cheese, and butter.[32] Additionally, it is a major building block of human milk oligosaccharides (HMOs), which suggests the potential application for producing HMOs such as Neu5Acα2−6Lac (6′SL) or Neu5Acα2−3Lac (3′SL).[33] It has been certified as a safe and functional additive material in food, which may further expand the application scope.[34] Chemical synthesis and simple extraction from natural materials for Neu5Ac preparation are usually accompanied by complicated procedures or low yield, which limit their widespread applications.[28] Enzymatic synthesis of Neu5Ac has the advantages of high yield and titer; Maru et al. obtained 625 mM Neu5Ac with a yield of 77% (mol/mol), but the requirement for ATP supplement increases the cost.[35] Microbial fermentation offers a greener and more sustainable approach to Neu5Ac synthesis, but the current Neu5Ac titer is low.[36] Therefore, economical and efficient processes for large-scale Neu5Ac production such as whole-cell catalysis are required to meet the increasing demands. While various attempts have been applied to Neu5Ac production, the titers (less than 412.6 mM) and productivities (slower than 15.9 g/(L h)) remain low with the present whole-cell systems.[37,38] In addition, side reactions and byproducts often exist during the Neu5Ac production partially due to the complexity of cellular metabolism.[39]

https://doi.org/10.1021/acs.jafc.3c07259
J. Agric. Food Chem. XXXX, XXX, XXX−XXX

This study proposes a thermal strategy for quickly developing high-performance whole-cell catalysis systems and verifies that with Neu5Ac as the target product. The strategy combines thermophilic enzymes, fast-growing *V. natriegens*, and high-temperature whole-cell catalysis. With this strategy, a high-performance Neu5Ac production system was built and optimized (Figure 1), whose productivity was more than 4.5-fold higher than the highest level reported. The complexity of cellular metabolism was simplified at the optimized high temperature, leading to a significant elimination of byproducts (60 °C).

MATERIALS AND METHODS

Strains, Plasmids, and Culture Conditions. The strain *Escherichia coli* BL21 (DE3) was used for protein expression, and *E. coli* DH5α was used for molecular cloning and vector propagation. *V. natriegens* Vmax (Synthetic Genomics, La Jolla, CA, USA) was used as the chassis for whole-cell catalysis. The expression plasmid pETDuet-1 was used for the cloning of PCR products. All of the constructed strains and plasmids are listed in Table S1.

For expressing AGE, the nucleotide sequences of *Acage* and *Txage* were synthesized after codon optimization for expression in *E. coli* and *V. natriegens*, and were inserted into pETDuet-1 with *Bam*HI and *Not*I, resulting in pETDuet-*Acage* and pETDuet-*Txage*, respectively.[38] For further producing Neu5Ac, the exogenously expressed *nanAs* were also synthesized after codon optimization, and the *EcnanA* was amplified using *E. coli* K12 genomic DNA.[40] All *nanAs* were inserted into pETDuet-*Txage* with *Kpn*I and *Xho*I. The resulting plasmids were transformed into *V. natriegens* Vmax or *E. coli* BL21 (DE3) as reported.[16] The recombinant strains *E. coli* BL21 (DE3) (pETDuet-*Txage-EcnanA*) and *V. natriegens* Vmax (pETDuet-*Txage-EcnanA*) were stored and deposited at the China Center for Type Culture Collection (CCTCC M 20221930 and CCTCC M 20221931, respectively). Primers used are listed in Table S2. Gene synthesis and DNA sequencing were performed by GENEWIZ (Suzhou, China).

The recombinant *E. coli* BL21 (DE3) was stored with 15% (v/v) glycerol stock at −20 °C and was incubated using LB broth (10 g/L tryptone, 5 g/L yeast extract, and 10 g/L NaCl) with the inoculation volume of 1% at 37 °C and 200 rpm. Recombinant *V. natriegens* Vmax was stored with 15% (v/v) glycerol stock at −80 °C and was incubated using LB3 broth (10 g/L tryptone, 5 g/L yeast extract, and 30 g/L NaCl) at 37 °C and 200 rpm. The concentration of ampicillin used was 100 μg/mL.

Chemicals. Unless otherwise noted, chemicals were purchased from Sangon Biotech (Shanghai, China). Tryptone and yeast extract were purchased from Oxoid (Basingstoke, England). PrimeSTAR Max DNA Polymerase (R045B) was purchased from Vazyme (Nanjing, China). The T4 DNA ligase and plasmid mini kit were purchased from Tiangen (Beijing, China). Isopropyl-D-thiogalactopyranoside (IPTG) was purchased from TaKaRa (Dalian, China).

Expression and Purification. When AGE or NanA was purified, recombinant *E. coli* BL21 (DE3) was preincubated overnight using 5 mL of LB broth at 37 °C and 200 rpm. Cultures were then transferred to a flask containing 1000 mL of LB broth and incubated at 37 °C, 200 rpm. Protein overexpression was induced by adding IPTG to a final concentration of 0.5 mM when the optical density measured at 600 nm (OD_{600}) reached between 0.6 and 0.8. Induction was performed at 16 °C for 16 h. After that, the cultures were centrifuged at 4600*g* for 20 min. The supernatant was discarded, and cells were resuspended with the phosphate buffer solution. The abovementioned process was repeated twice. The cells were then disrupted by the high-pressure homogenizer at 800−900 bar for 2 min (Antos Nano Technology, Suzhou, China). After that, cell lysates were centrifuged at 12,857*g* for 60 min at 4 °C, and the supernatant was filtered through a 0.22 μm filter. AGE or NanA with a hexahistidine tail at N-terminal ends was further purified using immobilized nickel−ion affinity chromatography. The purified proteins were analyzed with SDS-PAGE and stored in 100 mM Tris−HCl (pH 8) at −80 °C for further experiments. The entire purification process was performed at a low temperature to ensure the enzyme activity. Protein concentration was determined by NanoDrop (Thermo Scientific, Shanghai, China).

Enzyme Activity Determination. AGE activity was assayed by monitoring the formation of ManNAc from GlcNAc. The reaction mixture was composed of 100 mM Tris−HCl buffer, 10 mM $MgCl_2$, 50 mM GlcNAc, 1 mM ATP, and an appropriate amount of enzyme.[38] The reaction was performed at 37 °C and was terminated with 1/100 (v/v) hydrochloric acid after 2 min. The optimal temperature and pH of AGE were determined as above. The temperature ranged from 20 to 85 °C, and the pH ranged from 5 to 10.5. Kinetic assay of AGE was performed by changing the GlcNAc concentrations from 2 to 100 mM. Kinetic parameters were obtained by fitting these initial rates to the Michaelis−Menten equation using nonlinear regression.[41]

NanA activity was assayed by determining the formation of Neu5Ac from ManNAc.[40] The reaction was conducted with 100 mM Tris−HCl buffer, 50 mM ManNAc, 50 mM pyruvate, and an appropriate amount of enzyme. The reaction was terminated with 1/100 (v/v) hydrochloric acid after 10 min. The temperature ranged from 20 to 100 °C, and the pH ranged from 5 to 10.

Whole-Cell Catalysis Conditions. Recombinant *Vibrio* strains were preincubated overnight using 5 mL of LB3 broth at 37 °C and 200 rpm. Cultures were then transferred into a flask containing 1000 mL of LB3 broth and incubated at 37 °C, 200 rpm. Protein overexpression was induced by adding IPTG to a final concentration of 0.5 mM when the optical density measured at 600 nm (OD_{600}) reached between 0.6 and 0.8. Induction was performed at 37 °C for 4 h. After protein-induced expression, cells were collected by centrifuging at 2603*g* for 20 min, and the supernatant was discarded. Then, cells were resuspended in 30 mL phosphate buffer solution. The abovementioned process was repeated twice. The reaction mixture was composed of 100 mM Tris−HCl buffer (pH 7.5), 10 mM $MgCl_2$, 0.2−1.2 M GlcNAc, and 0.8−2 M pyruvate. The bioconversion reactions were performed in the 100 mL glass vessel (10 mL reaction system) at 65 or 60 °C and 200 rpm.

Analytical Methods. The sample was centrifuged at 13,523*g* for 5 min, and the supernatant was collected to determine the concentrations of Neu5Ac, ManNAc, and GlcNAc. The analysis was performed by an Agilent 1260 high-performance liquid chromatography (HPLC) (Agilent Technologies, shanghai, China) equipped with the RID detector and Bio-Rad aminex HPX-87H column (300 × 7.8 mm, BioRad Laboratories, Beverly, Mass). The mobile phase was 5 mM H_2SO_4, and the flow rate was 0.5 mL min^{-1}. The RID detector was at 35 °C, and the column oven was at 60 °C.

RESULTS AND DISCUSSION

Mining Thermophilic AGEs and NanAs. To establish high-performance biocatalysis for Neu5Ac at high temperatures, the first step includes mining thermophilic AGEs and NanAs. Thermophilic AGEs were mined with our previously developed tool CEM (http://cem.sjtu.edu.cn).[42] Using the amino acid sequence of the well-characterized *Anabaena* sp. CH1 AGE (acAGE, GeneBank: ABG57043.1) as a query; *Thermophagus xiamenensis* AGE (txAGE, GeneBank: WP_010526912.1) was ultimately selected as the best candidate.

Thermophilic NanA was mined through a combination of the CEM tool and bioinformatic calculation based on protein structures generated by AlphaFold2.[43] The amino acid sequence of ecNanA (GeneBank: KXH03056.1) was used as a query to seek potential candidates, and 92 proteins with high scores were selected. Subsequently, their putative structures were obtained using AlphaFold2 and molecular dockings were performed separately with GlcNAc and pyruvate, respectively.

https://doi.org/10.1021/acs.jafc.3c07259
J. Agric. Food Chem. XXXX, XXX, XXX−XXX

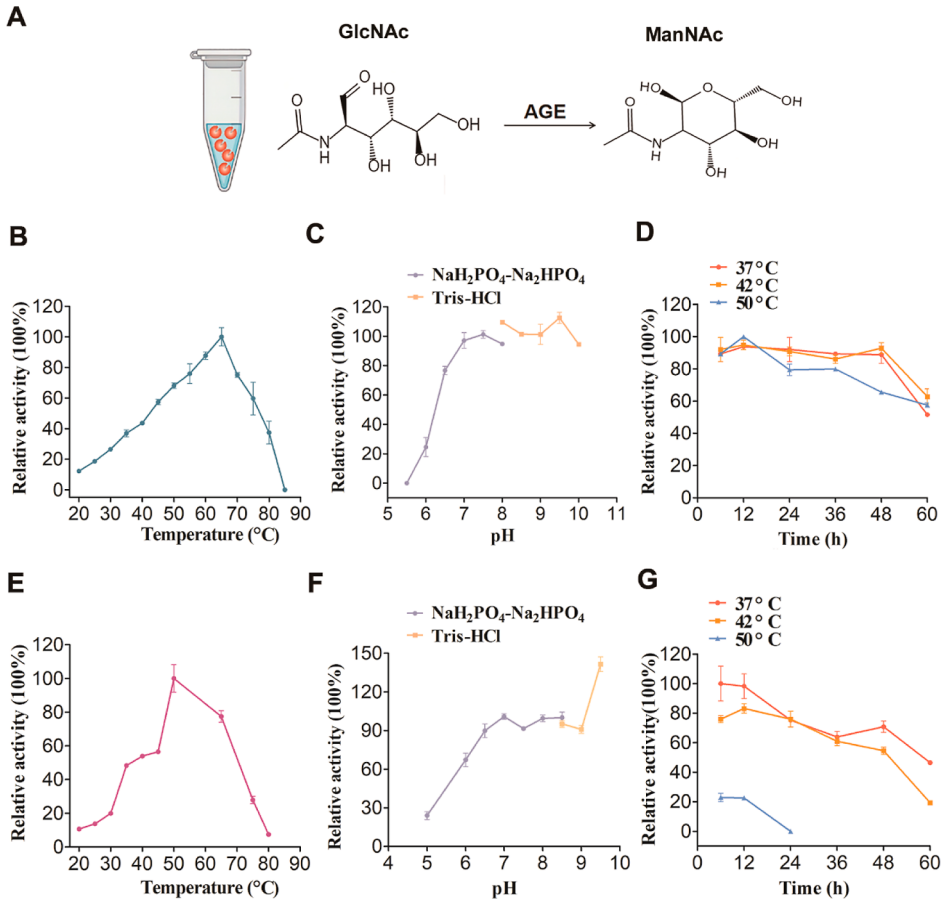

Figure 2. Activity assays of txAGE and acAGE. (A) Schematic diagram for ManNAc formation from GlcNAc with purified AGE. (B) The optimum temperature of txAGE. (C) The optimum pH of txAGE. (D) The thermal stability of txAGE. (E) The optimum temperature of acAGE. (F) The optimum pH of acAGE. (G) The thermal stability of acAGE. Triplicate experiments were done, and error bars represent the standard deviation.

The stability and aggregation propensity of these proteins were evaluated using FoldX and Aggrescan3D, respectively.[44,45] Specifically, the scores obtained from various approaches, including amino acid sequence identity, molecular docking energy, FoldX index, and Aggrescan3D index, were subjected to normalization and summation for scoring the candidates (Table S3). Thirteen candidate proteins were ultimately selected according to the calculated scores. Protein sequences of these candidates were then utilized to construct a phylogenetic tree through MEGA 7.0, and subsequently visualized using EvolView.[46,47] As the tree shows, *Sinorhizobium meliloti* NanA has the closest relationship to ecNanA and is in the same clade as *Ornithocaccomicrobium faecavium* NanA (Figure S1).

Verification of the Function of txAGE with Biocatalysis. Further, the catalysis function of txAGE was verified. *Txage* (the gene coding for txAGE) was expressed using pETDuet-1 with *E. coli* BL21(DE3). Then, whole-cell catalysis was performed with GlcNAc as the substrate. As shown in Figure S2, ManNAc was produced as time went on. To further investigate the function of txAGE, *Txage* and previously reported *EcnanA* (the gene coding for ecNanA) were both inserted in the plasmid pETDuet-1, resulting in pETDuet-*Txage-EcnanA*. The plasmid was transferred into *E. coli* BL21 (DE3) and then whole-cell catalysis was performed at 37 °C by optimizing the initial concentrations of pyruvate and GlcNAc. Initially, GlcNAc concentration was set at 0.2 M, whereas pyruvate was gradually increased to 0.8, 1.2, and finally to 1.6 M, respectively. At a pyruvate concentration of 1.6 M, the Neu5Ac titer reached 32.8 g/L after 24 h (Table S4). Next, different concentrations of GlcNAc (0.4 and 0.8 M) were employed with pyruvate at 1.6 M. After 24 h incubation, the highest Neu5Ac titer of 73.5 g/L was achieved with GlcNAc at 0.8 M and pyruvate at 1.6 M. Based on the results obtained, it can be concluded that txAGE was active and played a significant role in the whole-cell catalysis system for Neu5Ac synthesis.

Purification and Characterization of txAGE and acAGE. The enzymatic properties of txAGE were subsequently investigated. *Acage* (the gene coding for acAGE) and *Txage* (the gene coding for txAGE) were inserted in pETDuet-1, respectively. The resulting two plasmids were transferred into *E. coli* BL21 (DE3) for expressing and purifying the two AGEs. Successful expression of both proteins was confirmed by sodium dodecyl sulfate−polyacrylamide gel electrophoresis (SDS−PAGE) (Figure S3). The molecular masses of acAGE and txAGE were determined to be 42.4 and 42.3 kDa, respectively.

The purified txAGE and acAGE were further characterized in terms of their enzymatic properties (Figure 2A). The optimum temperature of txAGE was 65 °C (Figure 2B). Given that GlcNAc can undergo spontaneous conversion to ManNAc under alkaline conditions (pH > 9) without the need for enzymes, we did not consider the impact of alkaline pH (pH > 9) on the enzymatic activity when determining the optimal pH. Therefore, the optimum pH of txAGE was 8.0 (Figure 2C).

https://doi.org/10.1021/acs.jafc.3c07259
J. Agric. Food Chem. XXXX, XXX, XXX−XXX

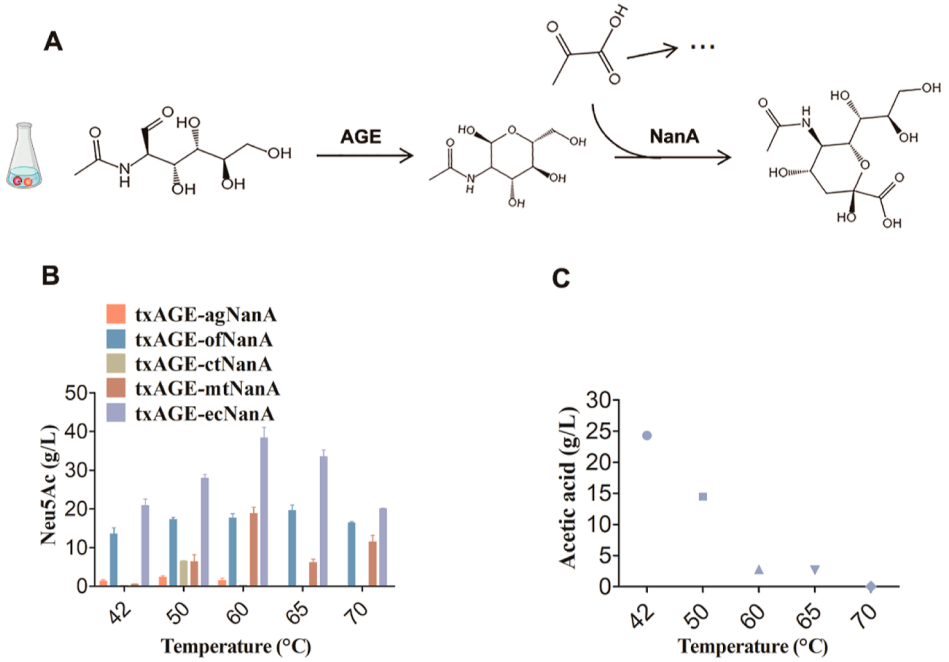

Figure 3. Comparison of the performance on Neu5Ac synthesis among different recombinant *Escherichia coli* BL21 (DE3) strains harboring txAGE and newly discovered thermophilic NanAs. The whole-cell catalysis reactions were performed at different temperatures for 24 h. The pyruvate and GlcNAc concentrations were 0.8 and 0.4 M, respectively. (A) The chemical process for Neu5Ac formation with whole-cell catalysis. (B) The performance of recombinant BL21 (DE3) strains harbor txAGE and newly discovered thermophilic NanAs at different temperature conditions. (C) The titers of acetic acid produced by BL21 (DE3) (pETDuet-*Txage-EcnanA*) at different temperature conditions after 24 h.

Approximately 90% of the initial activity was maintained at 37 and 42 °C for 48 h, while retaining 60% of the initial activity at 50 °C for the same duration. Moreover, the enzyme displayed remarkable stability even after 60 h, with more than 50% of the initial activities being retained under all three temperature conditions (Figure 2D). The optimum temperature of acAGE was 50 °C, and the optimum pH was 7.0 (Figure 2E,F). Compared with txAGE, acAGE exhibited inferior thermal stability. Incubation at 37 °C for 48 h resulted in a decrease of more than 20% in the relative activity of acAGE, while the activity of acAGE was found to be less than 60% at 42 °C for the same duration. After 60 h, roughly 50% of the initial activity was retained at 37 °C, while only approximately 20% of the initial activity remained at 42 °C. However, when exposed to 50 °C, the activity of the protein decreased rapidly, with only 20% residual activity detected after 6 h, and the reaction mixture became turbid. After 24 h, it was completely inactive (Figure 2G).

Kinetic analysis is shown in Table S5. The V_{max} of txAGE was 5.6 mM/min, the k_{cat} was 86.3 s^{-1}, and the K_m was 33.8 mM. The V_{max} of acAGE was 3.1 mM/min, the k_{cat} was 42.9 s^{-1}, and the K_m was 16.9 mM. These findings imply that txAGE possesses a higher catalytic efficiency than that of acAGE, indicating its potential to establish an effective Neu5Ac production system even at high temperatures.

Functional Verification of Thermophilic NanAs. Further, the function of all 13 NanA candidates in Neu5Ac synthesis was verified. Corresponding genes coding for them were inserted into pETDuet-*Txage*. Resulting plasmids were transferred to *E. coli* BL21 (DE3). In order to confirm the optimal reaction temperature of these strains, we conducted whole-cell catalysis with 0.8 M pyruvate and 0.4 M GlcNAc as substrates at a range of temperatures including 42, 50, 60, 65, and 70 °C, respectively (Figure 3A). Whole-cell catalysis with the strain *E. coli* BL21(DE3) (pETDuet-*Txage-EcnanA*) was also performed under the above temperature conditions.

Among these 13 proteins, four of them were validated to be active. However, the strain *E. coli* BL21(DE3) (pETDuet-*Txage-EcnanA*) exhibited superior performance under all experimental conditions tested. The Neu5Ac titer showed a remarkable improvement when exposed to temperatures ranging from 42 to 60 °C. The optimal temperature was found to be 60 °C, at which the Neu5Ac titer was the highest, 38.3 g/L after 24 h. When the temperature exceeded 60 °C, the performance of this strain decreased (Figure 3B). The superior performance of *E. coli* BL21(DE3) (pETDuet-*Txage-EcnanA*) was in agreement with bioinformatic calculations among the selected 13 NanAs with ecNanA, which showed that a low final parameter of calculations represents a potential thermophilic enzyme (Figure S4).

Except for this best strain, *E. coli* BL21 (DE3) (pETDuet-*Txage-OfnanA*) also displayed favorable performance with txAGE and ofNanA. The Neu5Ac titer reached its peak at 65 °C and was approximately 19.6 g/L after 24 h. Another good candidate was *Moorella thermoacetica* NanA. The strain *E. coli* BL21 (DE3) (pETDuet-*Txage-MtnanA*) produced Neu5Ac of approximately 18.8 g/L (60.9 mM) at 60 °C. However, when the temperature was higher or lower, the strain performance was inferior to that of *E. coli* BL21 (DE3) (pETDuet-*Txage-OfnanA*) (Figure 3B).

Further, the acetic acid titers produced by *E. coli* BL21(DE3) (pETDuet-*Txage-EcnanA*) were assessed at varying reaction temperatures. The formation of the byproduct acetic acid might partly be related to the chaos of cellular metabolism when the reaction temperature was below 70 °C. As shown in Figure 3C, The acetic acid titer exhibited a decreasing trend with increasing temperature, approximately 24.3 g/L at 42 °C and 2.8 g/L at 60 °C, a decrease of 88.5%.

https://doi.org/10.1021/acs.jafc.3c07259
J. Agric. Food Chem. XXXX, XXX, XXX−XXX

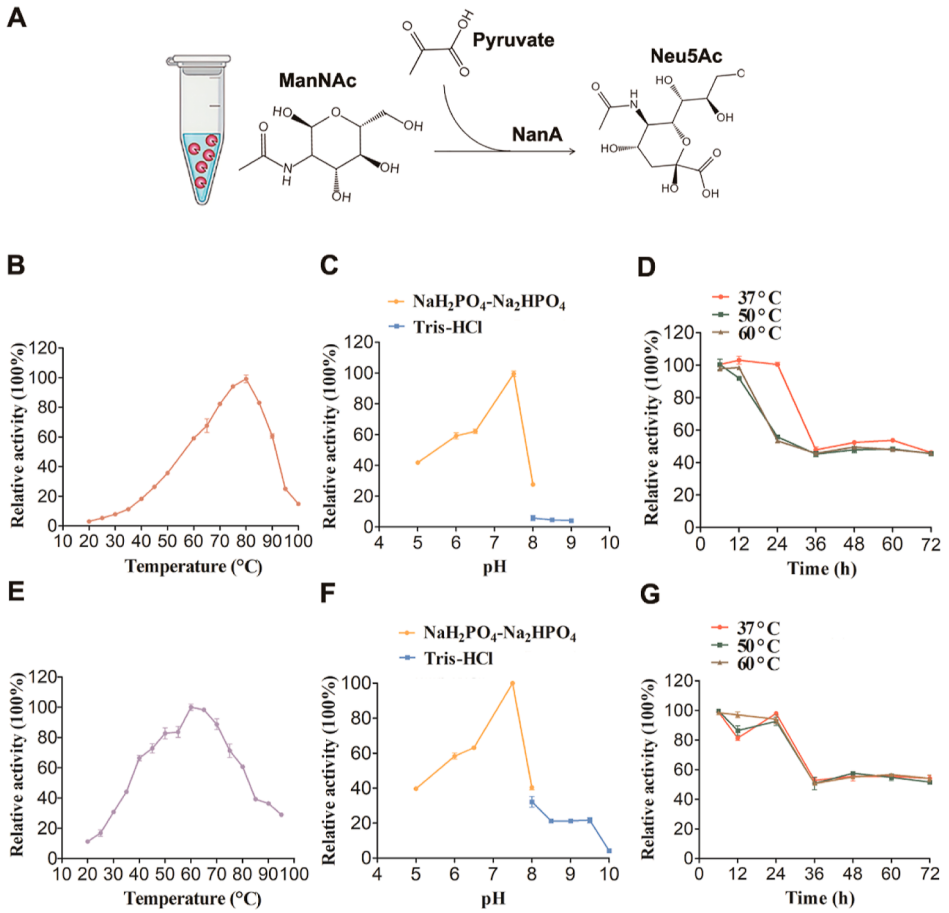

Figure 4. Activity assays of ofNanA and ecNanA. (A) The reaction for Neu5Ac formation from ManNAc and pyruvate with purified NanA. (B) The optimum temperature of ofNanA. (C) The optimum pH of ofNanA. (D) The thermal stability of ofNanA at 37 °C (filled circle), 50 °C (filled square), and 60 °C (filled triangle). (E) The optimum temperature of ecNanA. (F) The optimum pH of ecNanA. (G) The thermal stability of ecNanA at 37 °C (filled circle), 50 °C (filled square), and 60 °C (filled triangle). Triplicate experiments were done, and error bars represent standard deviation.

Thus, producing Neu5Ac with *E. coli* BL21(DE3) (pETDuet-*Txage-EcnanA*) or *E. coli* BL21(DE3) (pETDuet-*Txage-OfnanA*) at 60 or 65 °C was advantageous and could significantly reduce the formation of the byproduct acetic acid.

Notably, whole-cell catalysis with *E. coli* is usually carried out at mesophilic temperatures of 30 and 37 °C, preserving the cellular metabolic complexity similar to that of growing cells. Natural cellular enzymes inevitably compete with the desired pathways, necessitating their removal to enhance the yield, purity, and final titer of the target product.[25] Whole-cell catalysis at elevated temperatures far away from the optimal growth temperature of the host cells could potentially reduce the activities of endogenous enzymes, simplify the complexity of cellular metabolism, and result in the fewer side reactions and byproducts.[27] Here, the titer of the main byproduct acetic acid has resulted in a substantial 88.5% decrease with high-temperature whole-cell catalysis (Figure 3C), thereby enabling the goal of minimizing byproduct formation.

Purification and Characterization of ecNanA and ofNanA. The ecNanA and ofNanA were expressed with the strains *E. coli* BL21 (DE3) (pETDuet-*EcnanA*) and *E. coli* BL21 (DE3) (pETDuet-*OfnanA*), respectively. Then, they were purified, and the molecular masses of ecNanA and ofNanA were 32.5 and 32.2 kDa, respectively (Figure S5). They were then characterized in terms of their enzymatic properties (Figure 4A). The optimal temperature of ofNanA was 80 °C (Figure 4B), and the optimal pH was 7.5 (Figure 4C). After 24 h incubation, ofNanA presented approximately 100% of the initial activity at 37 °C, but its activity sharply decreased during the subsequent 24−36 h, leaving about 50% residual activity after 36 h. When incubated at higher temperatures of 50 and 60 °C, its activity decreased continuously during 12−36 h, with approximately 50% of initial activity remaining after 36 h. After incubation for 72 h, the residual activity was more than 40% of the initial activity under all of the detected conditions (Figure 4D). The optimal temperature of ecNanA was 60 °C (Figure 4E), and its optimal pH was 7.5 (Figure 4F). Its active pH range was broader than that of ofNanA. The ecNanA presented almost 100% of the initial activity within 24 h when incubated at 37, 50, and 60 °C, respectively. But the activity decreased rapidly during 24−36 h, and the residual activity was similar to that of ofNanA after 36 h under all three temperature conditions (Figure 4G). As described above, the active pH range was narrower, and the thermal stability was poorer than that of ecNanA, although the optimal temperature of ofNanA was higher than that of ecNanA.

To further investigate the abovementioned differences between the two NanAs, molecular dynamics simulations were then conducted. The protein structure of ofNanA was obtained from AlphaFold2, and the protein structure of ecNanA was obtained from the Protein Data Bank (PDB),

https://doi.org/10.1021/acs.jafc.3c07259
J. Agric. Food Chem. XXXX, XXX, XXX−XXX

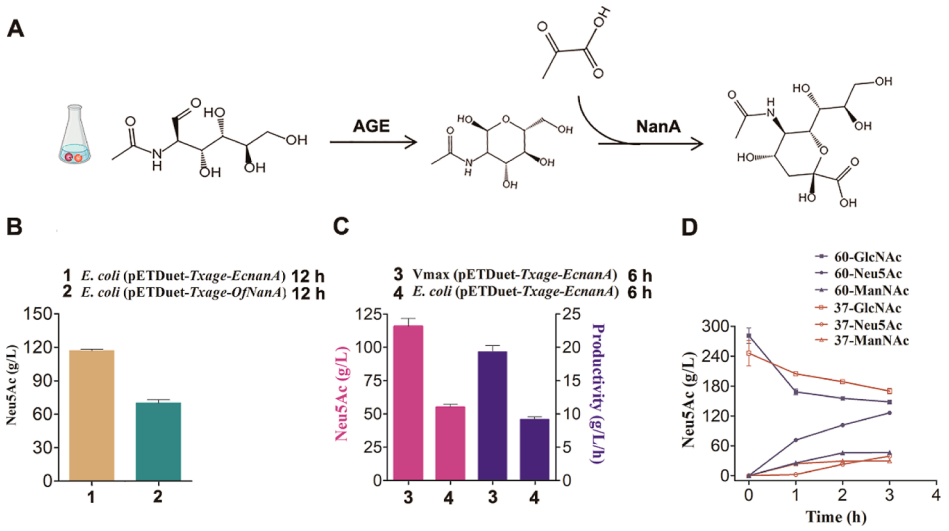

Figure 5. Establishment and optimization of high-temperature whole-cell catalysis system for Neu5Ac synthesis. The experiment was performed using a GlcNAc concentration of 1.2 M. For recombinant *V. natriegens*, protein-induced expression was performed at 37 °C for 4 h, whereas 16 °C for 16 h with recombinant *E. coli* strains. (A) Schematic diagram of the chemical process for Neu5Ac formation with whole-cell catalysis at high temperatures. (B) Whole-cell catalysis with *E. coli* BL21(DE3) (pETDuet-*Txage-EcnanA*) at 60 °C for 12 h (1) and *E. coli* BL21(DE3) (pETDuet-*Txage-OfnanA*) at 65 °C for 12 h (2). (C) Whole-cell catalysis with Vmax (pETDuet-*Txage-EcnanA*) at 60 °C for 6 h (3) and *E. coli* BL21(DE3) (pETDuet-*Txage-EcnanA*) at 60 °C for 6 h (4). (D) Time course of biocatalysis with Vmax (pETDuet-*Txage-EcnanA*) at 60 and 37 °C for 3 h.

accession number at 3LBM. Additionally, the structure of ManNAc was downloaded from the ZINC database (http://zinc.docking.org/),[48] accession number ZINC4228290. Next, molecular dockings were performed with LeDock software,[49] resulting complexes of ofNanA-ManNAc and ecNanA-ManNAc (Figure S6). Then, the complexes were used to perform molecular dynamics simulations at 300 K and 50 ns with Gromacs software.[50] As shown in Figure S7, the proteins and the ligand remained stable between 10 and 50 ns. Further, molecular mechanics generalized born surface area (MM/GBSA) binding free energy calculations were performed based on the results of molecular dynamics simulations (Figure S8).[51] The binding free energy of ofNanA-ManNAc was −4.0 kcal/mol, whereas that of ecNanA-ManNAc was −5.9 kcal/mol. These results suggest that ecNanA is more rigid in its binding to ManNAc than it is to ofNanA, which aligns with its better thermal stability and broad pH adaptability compared to those of ofNanA.

Biocatalysis Optimization with txAGE-ofNanA and txAGE-ecNanA. To improve the performance of the txAGE-ofNanA-coupled whole-cell catalysis system at 65 °C (protein-induced expression at 16 °C for 16 h), we conducted experiments to measure the impact of different GlcNAc concentrations while maintaining a pyruvate concentration of 1.6 M (Figures 5A and S9A). At a GlcNAc concentration of 0.8 M (177.0 g/L), the Neu5Ac titer was 91.1 g/L after 24 h with the productivity of 3.8 g/(L h). The maximum titer of Neu5Ac reached 105.2 g/L with the productivity of 4.4 g/(L h) at a GlcNAc concentration of 1 M (221.2 g/L). At a GlcNAc concentration of 1.2 M (265.5 g/L), the maximum titer of Neu5Ac reached 70.3 g/L after 12 h (Figure 5B) and 107.1 g/L after 24 h (Figure S9A).

For the strain *E. coli* BL21 (DE3) (pETDuet-*Txage-EcnanA*), after protein-induced expression at 16 °C for 16 h, the reaction was conducted at 60 °C and 200 rpm. With pyruvate and GlcNAc of 1.6 and 1.2 M, respectively, the Neu5Ac titer reached 117.0 g/L after 12 h, with the productivity of 9.8 g/(L h) (Figures 5B and S9B). Thus, the txAGE-ecNanA-coupled whole-cell catalysis system was superior to the txAGE-ofNanA-coupled system when both NanAs were working at their respective optimal temperatures. Moreover, protein-induced expression at 37 °C for 6 h and 28 °C for 6 h was also attempted to improve Neu5Ac titer.[37] As shown in Figure S9B, although the reaction rates at the early stage are different under different protein-induced conditions, the Neu5Ac titers were similar in the initial 12 h. When induction was at 28 °C for 6 h, the Neu5Ac titer was 119.3 g/L after 12 h with a corresponding productivity of 9.9 g/(L h), and the final Neu5Ac titer reached 131.6 g/L after 24 h. When induction was at 37 °C for 6 h, the Neu5Ac titer was 117.8 g/L, the corresponding productivity was 9.8 g/(L h), and the final titer was 125.6 g/L after 24 h (Figure S9B).

Notably, ecNanA from *E. coli*, which is commonly utilized for Neu5Ac production, exhibits a high optimal temperature of 60 °C (Figure 4E). However, the reactions were previously performed at 30 °C or 37 °C as reported,[37] amounting to less than 50% of its maximum activity. Here, by implementing our thermal strategy at 60 °C, the ecNanA performance was maximized. Furthermore, despite *E. coli* being classified as a mesophilic bacterium, ecNanA demonstrated significant efficacy at 60 °C, consistent with the bioinformatic calculations (Figure S4). It also strongly suggests that mesophilic species should be considered for mining thermophilic enzymes and emphasizes the importance of accurate bioinformatic calculations.

Rapid Biocatalysis with Fast-Growing *V. natriegens*. As reported, *V. natriegens* is a fast-growing genus and has proven to be effective in protein expression.[16] Consequently, it is considered to be a promising candidate for facilitating whole-cell catalysis for synthesizing valuable compounds. To further enhance the performance of Neu5Ac synthesis system, *V. natriegens* was employed.

Specifically, the plasmid pETDuet-*Txage-EcnanA* was introduced into *V. natriegens* Vmax, resulting in *V. natriegens* Vmax (pETDuet-*Txage-EcnanA*). Protein-induced expression was conducted at 37 °C for 4 h.[21] Surprisingly, the reactions

https://doi.org/10.1021/acs.jafc.3c07259
J. Agric. Food Chem. XXXX, XXX, XXX−XXX

performed beyond our expectation. As shown in Figure 5C, at concentrations of 1.6 M for pyruvate and 1.2 M for GlcNAc, the maximum Neu5Ac titer of 115.7 g/L was achieved at 6 h, with an average productivity of 19.3 g/(L h), twice as high as that of *E. coli* BL21(DE3) (pETDuet-*Txage-EcnanA*) in the same reaction time (Figure 5C). Within the initial 2 h, the productivity reached 34.3 g/(L h). However, Neu5Ac titer decreased after 6 h, and this phenomenon of decreasing titers after reaching the peak also appeared in other studies.[52] At concentrations of 1.6 M for pyruvate and 1 M for GlcNAc, the maximum Neu5Ac titer was 111.8 g/L after 6 h, and the average productivity reached 18.6 g/(L h). Within the initial 2 h, the productivity reached 27.4 g/(L h) (Figure S9C).

Further, we increased the concentration of pyruvate to 2.0 M (Figure 5D). The efficiency was significantly improved than that of 1.6 M. At a GlcNAc concentration of 1.2 M, the Neu5Ac titer was the maximum at 3 h, reaching 126.1 g/L with an average productivity of 42.0 g/(L h), a yield of 34.1% (mol/mol), and an initial first-hour productivity of 71.6 g/L/h. We also conducted this experiment at 37 °C. As shown in Figure 5D, only 39.2 g/L Neu5Ac was produced after 3 h. Undoubtedly, high-temperature biocatalysis exhibited remarkable superiority over that of moderate-temperature biocatalysis for Neu5Ac synthesis. Furthermore, we compared the protein expression between *E. coli* BL21 (DE3) (pETDuet-*Txage-EcnanA*) (37 °C for 6 h and 28 °C for 6 h) and *V. natriegens* Vmax (pETDuet-*Txage-EcnanA*) (37 °C for 4 h), the latter exhibited even higher protein production than the former although in a shorter time frame, which may relate to better performance of *V. natriegens* Vmax (pETDuet-*Txage-EcnanA*) than that of *E. coli* BL21 (DE3) (pETDuet-*Txage-EcnanA*) (Figure S10).

With the thermal strategy, we achieved the Neu5Ac productivity of 71.6 g/(L h) in the first hour, more than 4.5-fold higher than the highest reported (Table S6).[37] Some factors may contribute to the high-performance production of Neu5Ac in this study. High-temperature catalysis offers high reaction rates, suggested by the Arrhenius equation, and has been studied extensively by researchers.[53] The average Neu5Ac productivity produced by *V. natriegens* Vmax (pETDuet-*Txage-EcnanA*) at 60 °C was almost 3-fold higher than that at 37 °C (Figure 5D). It is reasonable to conclude that the remarkable high-performance production of Neu5Ac was attained by employing high-temperature catalysis with thermophilic enzymes, possessing exceptional catalytic activity at elevated temperatures. Since the productivity of *V. natriegens* Vmax (pETDuet-*Txage-EcnanA*) was almost twice that of the *E. coli* (pETDuet-*Txage-EcnanA*) (Figure 5C), the application of *V. natriegens* could be another key factor in achieving the efficient Neu5Ac production. The cell volume of *V. natriegens* is notably smaller than that of *E. coli*, measuring approximately 0.93 μm^3 $cell^{-1}$.[54] This endows it a large specific surface area, which may facilitate the substance transportation and ultimately improve the reaction rate.[21] As previously reported, the integrity of cell membrane and cell wall is partly reduced at high temperatures, which may enhance the permeability and promote the reaction by improving accessibility between the enzymes and substrates.[55] To investigate this issue, we assessed the cell membrane permeability at both 60 °C and 37 °C,[56] and observed a little increase in membrane permeability when the temperature was elevated to 60 °C, which may promote the reaction at high-temperatures (Figure S11). Besides, viscosity of the reaction mixture is usually encountered in biocatalysis, which is shown in the catalysis system of *V. natriegens*.[57] High viscosity often makes the reaction mixture difficult to mix sufficiently, influencing mass transfer and finally hindering the reaction. With our thermal strategy, the viscosity decreased under high temperatures, which may contribute to the improved mass transfer, titer, and productivity.[58] In summary, these multiple factors may synergistically contribute to the high-performance production of Neu5Ac in our high-temperature whole-cell catalysis.

Reducing Metabolic Chaos by Exposing Cells in High Temperature. As mentioned above, the titer of the byproduct acetic acid was significantly decreased at elevated temperatures. This phenomenon could potentially be attributed to simplification of the natural complexity of cellular metabolism at high temperatures, leading to diminished side reactions and corresponding byproducts. To substantiate this assertion, we performed protein T_m index (melting temperature) calculations on the overall proteomic levels of *E. coli* K12 (Figure 6A). The T_m indexes of phosphate acetyltransferase (UniProt number: P0A9M8) and acetate kinase (UniProt number: PA06A3) in acetic acid synthesis pathways were 0.4 and 1.0, respectively, while the T_m index of txAGE was 1.5, which was much higher than those of the two critical enzymes in acetic acid synthesis pathways. Furthermore, a majority of intracellular proteins (85.4%) displayed lower T_m indexes when

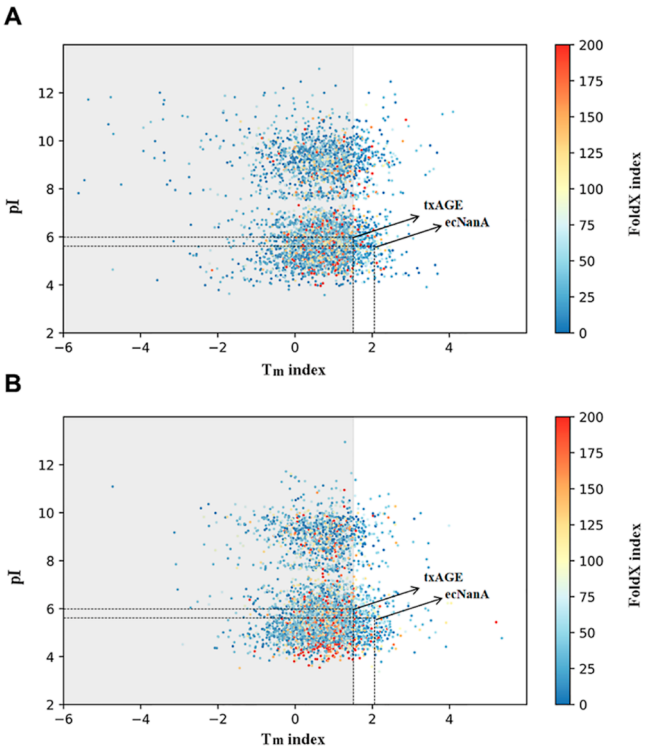

Figure 6. The thermal stability analysis of proteins in *Escherichia coli* K12 and *Vibrio natriegens* at the overall proteomic levels. The analysis included calculating the pI (isoelectric point), T_m index (melting temperature index), and FoldX index (free energy calculation by the FoldX software) of each protein. The resulting data set was plotted as colorful dots on a coordinate system, where the color of the dot reflected the approximate range of the FoldX value. Proteins in gray areas mean that their T_m indexes are less than that of txAGE. (A) The thermal stability analysis of proteins on the overall proteomic level of *E. coli* K12. (B) The thermal stability analysis of proteins on the overall proteomic level of *V. natriegens*.

https://doi.org/10.1021/acs.jafc.3c07259
J. Agric. Food Chem. XXXX, XXX, XXX−XXX

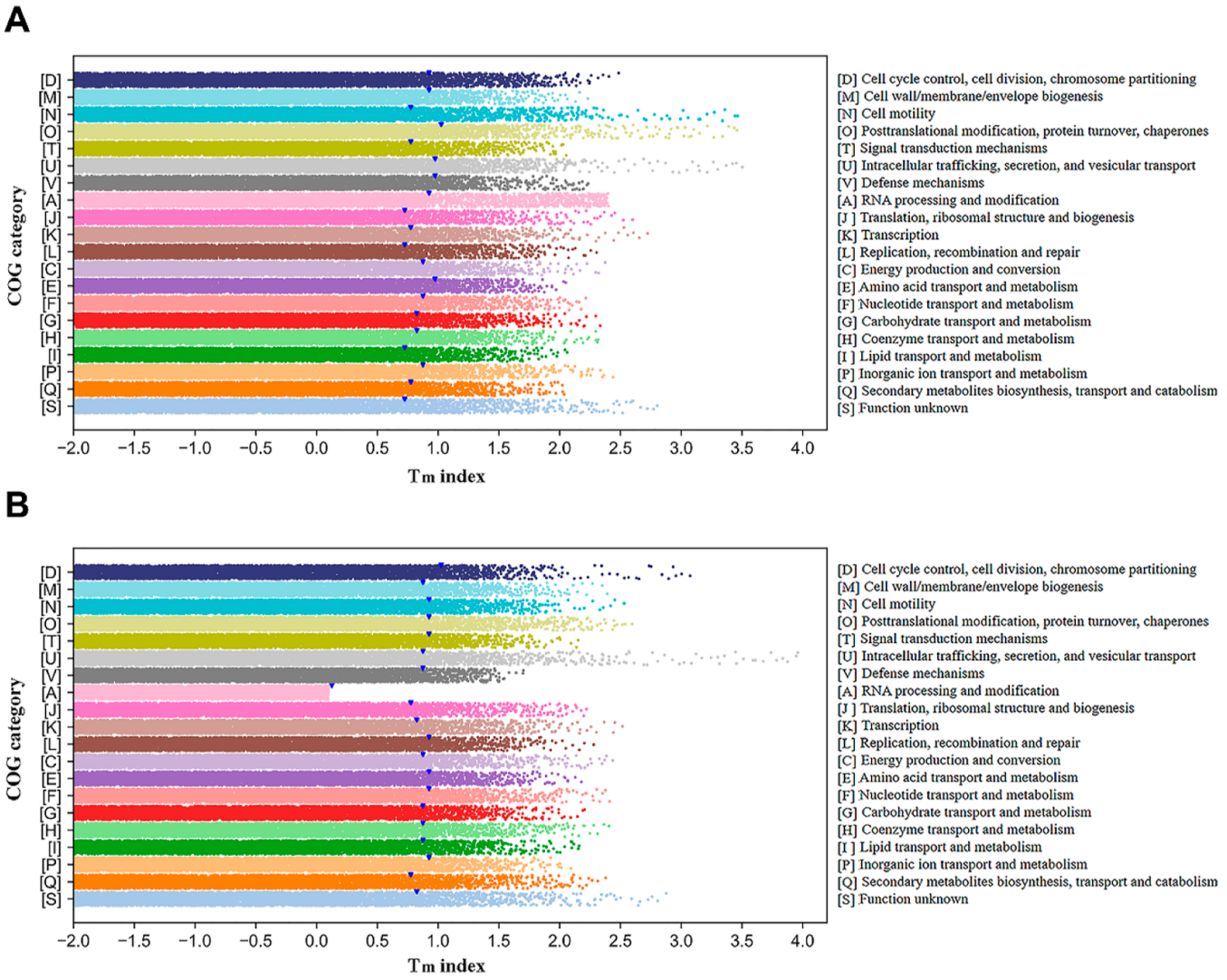

Figure 7. Thermal stability analysis of cellular functional systems in *E. coli* K12 and *V. natriegens* based on COG classification at the overall proteomic levels. Proteins were classified in 20 COG categories. The dot density represents the percentage of proteins that remain active in the functional system, and proteins with higher T_m indexes than the corresponding T_m index value on the *X* axis are considered active. The median T_m index value for each functional system is marked by an inverted triangle. (A) The thermal stability analysis of cellular functional systems on the overall proteomic level of *E. coli* K12. (B) The thermal stability analysis of cellular functional systems on the overall proteomic level of *V. natriegens*.

compared to that of txAGE [Figure 6A and additional file 1 (Supporting Information)]. To verify the generalizability of this phenomenon, we also performed an overall T_m index calculations with the emerging next-generation chassis *V. natriegens*. There are four annotated enzymes related to acetic acid synthesis, and their T_m indexes were 1.5 (acetate kinase, UniProt number: A0A1B1ECS6), 1.0 (acetate kinase; UniProt number: A0A1B1EJM9), 1.2 (acetate kinase, UniProt number: A0A1B1EDJ3), and 0.2 (phosphateacetyltransferase; UniPort number: A0A1B1EDI1), respectively. Besides, 86.8% of intracellular proteins' T_m indexes were lower than that of txAGE (UniProt number: A0A1I1USR1) [Figure 6B and Additional File 1 (Supporting Information)]. These characteristics are in line with those reported by Chang, and strongly suggest that our strategy of elevating reaction temperature is promising to solve byproduct problems by inactivating the undesired pathway enzymes.[59] Moreover, our strategy may have universal applicability for eliminating the byproducts when synthesizing other valuable compounds. In addition, we analyzed the T_m indexes of ATP synthase subunits in *V. natriegens* and *E. coli* K12. There are 5 enzymes (UniProt number and T_m index: A0A1B1EJF7 1.6, A0A1B1EJC8 1.8, A0A1B1EK30 2.4, A0A1B1EG78 1.7, and A0A1B1EJN7 2.9) with higher T_m indexes than that of txAGE in *V. natriegens*, while only three annotated ATP synthase subunits are higher than that of txAGE in *E. coli* (UniProt number and T_m index: P0ABC0 2.6, P0ABB4 1.6, and P68699 2.3), meaning that it is possibly more sufficient in *V. natriegens* to supply cofactor ATP in the txAGE catalysis step (additional file 1 (Supporting Information)].

The abovementioned observation inspired us to investigate whether exposing cells to high temperatures could gradually disrupt their metabolic network in specific patterns, which the understanding may enable rational engineering of cells for production with biotechnology. To address this gap in knowledge, we classified *E. coli* and *V. natriegens* proteins into 20 functional categories (functional systems) based on the clusters of orthologous groups (COG) database. Then, we calculated the rates of residual active proteins for each cellular functional system as the T_m index increased. The medians of

https://doi.org/10.1021/acs.jafc.3c07259
J. Agric. Food Chem. XXXX, XXX, XXX−XXX

the T_m index values in the corresponding cellular functional system were also calculated, which signify a collapsing point of the respective cellular functions (Figure 7). In *E. coli* K12, the initial disintegrated systems are related to replication, translation, and lipid transport; following systems are related to cell motility, signal transduction, transcription, and secondary metabolism, while the final broken system is correlated with posttranslational modification (Figure 7A).

In *V. natriegens*, the primary disintegrated systems are related to RNA processing and modification, following the systems for secondary metabolism and protein synthesis, and for cell cycle control and division (Figure 7B). It suggests that as the fastest-growing bacterium, *V. natriegens* prioritizes cell survival by abandoning protein synthesis functions first when exposed to high temperatures. While *E. coli* seems to first abandon the important cell process for survival such as cell replication. This suggests that different genera may exhibit varying reactions to the high-temperature exposure. We also noted that *V. natriegens* displays greater resilience in proteins responsible for intracellular trafficking and secretion than *E. coli* K12 at high temperatures, potentially contributing to rapid Neu5Ac synthesis using our system. All these differences suggest that reducing metabolic chaos is intriguing through high-temperature exposure, and further intensive study may be fruitful in the future.

In this study, a powerful thermal strategy has been proposed to realize high-performance whole-cell biocatalysis and it has been successfully applied to Neu5Ac synthesis. The strategy combines fast-growing *V. natriegens*, thermophilic enzymes, and high-temperature catalysis, resulting in a whole-cell catalysis system that capable of efficiently producing Neu5Ac at elevated temperatures. It produced an impressive concentration of Neu5Ac (126.1 g/L) with a productivity (71.6 g/(L h)) nearly 7.2-fold higher than that of *E. coli*. Moreover, the final concentration of byproduct acetic acid was effectively eliminated, accompanied by a reduction in the complexity of cellular metabolism. With our strategy, the entire process (including early stage growth, protein expression, and reaction) can be completed within 10 h, which is almost 2-fold faster than the best-reported result. This study establishes an effective strategy for rapid Neu5Ac production and opens up new avenues for the future food industry.

■ ASSOCIATED CONTENT

Supporting Information

The Supporting Information is available free of charge at https://pubs.acs.org/doi/10.1021/acs.jafc.3c07259.

The methods for mining thermophilic enzymes, T_m index calculation and visualization of proteins, molecular docking, molecular dynamics simulation, and MM−GBSA binding free energy calculation; the scripts for downloading protein information from the UniProt web site, automatic calculations for pI values, T_m indexes, and FoldX indexes, phylogenetic tree of thermophilic NanAs, whole-cell catalysis for ManNAc production with txAGE, protein expression determination of AGEs, the bioinformatic calculation parameters of NanAs, protein expression determination of NanAs, molecule docking of ofNanA and ecNanA with the ligand ManNAc, rmsd values and MM/GBSA binding free energy calculation of the ofNanA-ManNAc and ecNanA-ManNAc, the high-temperature whole-cell catalysis system for Neu5Ac synthesis by different recombinant strains, comparison of protein expression between recombinant *E. coli* and *V. natriegens*, membrane permeability determination, information on strains, plasmids, and primers, information on thermophilic NanAs mined in this work, effect of substrate concentrations on the Neu5Ac synthesis, the kinetic parameters of acAGE and txAGE, comparison of Neu5Ac synthesis capability by different biocatalysts (PDF)

■ AUTHOR INFORMATION

Corresponding Authors

Ping Xu − *State Key Laboratory of Microbial Metabolism, Joint International Research Laboratory of Metabolic and Developmental Sciences, and School of Life Sciences and Biotechnology, Shanghai Jiao Tong University, Shanghai 200240, People's Republic of China*; orcid.org/0000-0002-4418-9680; Phone: +86-21-34206647; Email: pingxu@sjtu.edu.cn

Fei Tao − *State Key Laboratory of Microbial Metabolism, Joint International Research Laboratory of Metabolic and Developmental Sciences, and School of Life Sciences and Biotechnology, Shanghai Jiao Tong University, Shanghai 200240, People's Republic of China*; Email: taofei@sjtu.edu.cn

Authors

Yuan Peng − *State Key Laboratory of Microbial Metabolism, Joint International Research Laboratory of Metabolic and Developmental Sciences, and School of Life Sciences and Biotechnology, Shanghai Jiao Tong University, Shanghai 200240, People's Republic of China*

Lina Ma − *State Key Laboratory of Microbial Metabolism, Joint International Research Laboratory of Metabolic and Developmental Sciences, and School of Life Sciences and Biotechnology, Shanghai Jiao Tong University, Shanghai 200240, People's Republic of China*

Complete contact information is available at: https://pubs.acs.org/10.1021/acs.jafc.3c07259

Author Contributions

P.X. and F.T. conceived the projects, F.T., P.X., and Y.P. designed the experiments, Y.P. performed the experiments and wrote the original draft, and F.T., P.X., and Y.P. revised the manuscript. L.M. performed the calculations of molecular dynamics simulations and MM/GBSA binding free energy.

Funding

This study is supported by the grant from National Natural Science Foundation of China (22138007 and 32170105).

Notes

The authors declare no competing financial interest.

■ REFERENCES

(1) Clarke, L.; Kitney, R. Developing synthetic biology for industrial biotechnology applications. *Biochem. Soc. Trans.* **2020**, *48*, 113−122.

(2) Agapakis, C. M. Designing synthetic biology. *ACS Synth. Biol.* **2014**, *3*, 121−128.

(3) Tan, C.; Xu, P.; Tao, F. Harnessing interactional sensory genes for rationally reprogramming chaotic metabolism. *Research* **2022**, *2022*, 0017.

(4) Datsenko, K. A.; Wanner, B. L. One-step inactivation of chromosomal genes in *Escherichia coli* K-12 using PCR products. *Proc. Natl. Acad. Sci. U. S. A.* **2000**, *97*, 6640−6645.

https://doi.org/10.1021/acs.jafc.3c07259
J. Agric. Food Chem. XXXX, XXX, XXX−XXX

(5) Cho, S.; Shin, J.; Cho, B. K. Applications of CRISPR/Cas system to bacterial metabolic engineering. *Int. J. Mol. Sci.* **2018**, *19*, 1089.
(6) Xin, B.; Tao, F.; Wang, Y.; Liu, H.; Ma, C.; Xu, P. Coordination of metabolic pathways: enhanced carbon conservation in 1,3-propanediol production by coupling with optically pure lactate biosynthesis. *Metab. Eng.* **2017**, *41*, 102−114.
(7) Song, P.; Zhang, X.; Wang, S.; Xu, W.; Wei, F. Advances in the synthesis of β-alanine. *Front. Bioeng. Biotechnol.* **2023**, *11*, 1283129.
(8) Wu, M.; Jiang, Y.; Liu, Y.; Mou, L.; Zhang, W.; Xin, F.; Jiang, M. Microbial application of thermophilic *Thermoanaerobacterium* species in lignocellulosic biorefinery. *Appl. Microbiol. Biotechnol.* **2021**, *105*, 5739−5749.
(9) Dumorne, K.; Cordova, D. C.; Astorga-Elo, M.; Renganathan, P. Extremozymes: a potential source for industrial applications. *J. Microbiol. Biotechnol.* **2017**, *27*, 649−659.
(10) Wang, P.; Wang, P.; Tian, J.; Yu, X.; Chang, M.; Chu, X.; Wu, N. A new strategy to express the extracellular alpha-amylase from *Pyrococcus furiosus* in *Bacillus amyloliquefaciens*. *Sci. Rep.* **2016**, *6*, 22229.
(11) Gopinath, S. C. B.; Anbu, P.; Arshad, M. K. M.; Lakshmipriya, T.; Voon, C. H.; Hashim, U.; Chinni, S. V. Biotechnological processes in microbial amylase production. *Biomed. Res. Int.* **2017**, *2017*, 1272193.
(12) van den Burg, B. Extremophiles as a source for novel enzymes. *Curr. Opin. Microbiol.* **2003**, *6*, 213−218.
(13) Eagon, R. G. *Pseudomonas natriegens*, a marine bacterium with a generation time of less than 10 minutes. *J. Bacteriol.* **1962**, *83*, 736−737.
(14) Austin, B.; Zachary, A.; Colwell, R. R. Recognition of *Beneckea natriegens* (Payne et al.) Baumann et al. as a member of the genus *Vibrio*, as previously proposed by Webb and Payne. *Int. J. Syst. Bacteriol.* **1978**, *28*, 315−317.
(15) Payne, W. J. Studies on bacterial utilization of uronic acids III. induction of oxidative enzymes in a marine isolate. *J. Bacteriol.* **1958**, *76*, 301−307.
(16) Weinstock, M. T.; Hesek, E. D.; Wilson, C. M.; Gibson, D. G. *Vibrio natriegens* as a fast-growing host for molecular biology. *Nat. Methods* **2016**, *13*, 849−851.
(17) Xu, J.; Yang, S.; Yang, L. *Vibrio natriegens* as a host for rapid biotechnology. *Trends Biotechnol.* **2022**, *40*, 381−384.
(18) Hoffart, E.; Grenz, S.; Lange, J.; Nitschel, R.; Müller, F.; Schwentner, A.; Feith, A.; Lenfers-Lücker, M.; Takors, R.; Blombach, B. High substrate uptake rates empower *Vibrio natriegens* as production host for industrial biotechnology. *Appl. Environ. Microbiol.* **2017**, *83*, No. e01614-17.
(19) Meng, W.; Zhang, Y.; Ma, L.; Lu, C.; Xu, P.; Ma, C.; Gao, C. Non-Sterilized fermentation of 2,3-Butanediol with seawater by metabolic engineered fast-growing *Vibrio natriegens*. *Front. Bioeng. Biotechnol.* **2022**, *10*, 955097.
(20) Zhang, Y.; Li, Z.; Liu, Y.; Cen, X.; Liu, D.; Chen, Z. Systems metabolic engineering of *Vibrio natriegens* for the production of 1,3-propanediol. *Metab. Eng.* **2021**, *65*, 52−65.
(21) Liu, X.; Han, X.; Peng, Y.; Tan, C.; Wang, J.; Xue, H.; Xu, P.; Tao, F. Rapid production of I-DOPA by *Vibrio natriegens*, an emerging next-generation whole-cell catalysis chassis. *Microb. Biotechnol.* **2022**, *15*, 1610−1621.
(22) Jiang, C.; Liu, X.; Chen, X.; Cai, Y.; Zhuang, Y.; Liu, T.; Zhu, X.; Wang, H.; Liu, Y.; Jiang, H.; Wang, W. Raising the production of phloretin by alleviation of by-product of chalcone synthase in the engineered yeast. *Sci. China: Life Sci.* **2020**, *63*, 1734−1743.
(23) Huang, K.; Zhang, B.; Shen, Z.; Cai, X.; Liu, Z.; Zheng, Y. G. Enhanced amphotericin B production by genetically engineered *Streptomyces nodosus*. *Microbiol. Res.* **2021**, *242*, 126623.
(24) Zou, S.; Wang, Z.; Zhao, K.; Zhang, B.; Niu, K.; Liu, Z.; Zheng, Y. High-level production of d-pantothenic acid from glucose by fed-batch cultivation of *Escherichia coli*. *Biotechnol. Appl. Biochem.* **2021**, *68*, 1227−1235.
(25) Lin, B.; Tao, Y. Whole-cell biocatalysts by design. *Microb. Cell Fact.* **2017**, *16*, 106.
(26) Lin, B. X.; Zhang, Z. J.; Liu, W. F.; Dong, Z. Y.; Tao, Y. Enhanced production of *N*-acetyl-d-neuraminic acid by multi-approach whole-cell biocatalyst. *Appl. Microbiol. Biotechnol.* **2013**, *97*, 4775−4784.
(27) Ninh, P. H.; Honda, K.; Yokohigashi, Y.; Okano, K.; Omasa, T.; Ohtake, H. Development of a continuous bioconversion system using a thermophilic whole-cell biocatalyst. *Appl. Environ. Microbiol.* **2013**, *79*, 1996−2001.
(28) Yang, H.; Lu, L.; Chen, X. An overview and future prospects of sialic acids. *Biotechnol. Adv.* **2021**, *46*, 107678.
(29) Wu, W.; Air, G. M. Binding of influenza viruses to sialic acids: reassortant viruses with A/NWS/33 hemagglutinin bind to alpha 2,8-linked sialic acid. *Virology* **2004**, *325*, 340−350.
(30) Bondioli, L.; Ruozi, B.; Belletti, D.; Forni, F.; Vandelli, M. A.; Tosi, G. Sialic acid as a potential approach for the protection and targeting of nanocarriers. *Expert Opin. Drug Delivery* **2011**, *8*, 921−937.
(31) Wang, B. Sialic acid is an essential nutrient for brain development and cognition. *Annu. Rev. Nutr.* **2009**, *29*, 177−222.
(32) Karunanithi, D.; Radhakrishna, A.; Biju, V. M. Quantitative determination of sialic acid in Indian milk and milk products. *Int. J. Appl. Biol. Pharm. Technol.* **2013**, *4*, 318−323.
(33) Chen, X. Human Milk Oligosaccharides (HMOS): Structure, Function, and Enzyme-Catalyzed Synthesis. *Adv. Carbohydr. Chem. Biochem.* **2015**, *72*, 113−190.
(34) Röhrig, C. H. *GRAS exemption claim for N-acetyl-d-neuraminic acid (NANA). GRAS Notice 602*, 2015.
(35) Maru, I.; Ohnishi, J.; Ohta, Y.; Tsukada, Y. Simple and large-scale production of *N*-acetylneuraminic acid from *N*-acetyl-d-glucosamine and pyruvate using *N*-acyl-d-glucosamine 2-epimerase and *N*-acetylneuraminate lyase. *Carbohydr. Res.* **1998**, *306*, 575−578.
(36) Liu, C.; Lv, X.; Li, J.; Liu, L.; Du, G.; Liu, Y. Metabolic engineering of *Escherichia coli* for increased bioproduction of *N*-acetylneuraminic acid. *J. Agric. Food Chem.* **2022**, *70*, 15859−15868.
(37) Kao, C. H.; Chen, Y. Y.; Wang, L. R.; Lee, Y. C. Production of *N*-acetyl-d-neuraminic acid by recombinant single whole cells co-expressing *N*-acetyl-d-glucosamine-2-epimerase and *N*-acetyl-d-neuraminic acid aldolase. *Mol. Biotechnol.* **2018**, *60*, 427−434.
(38) Lee, Y. C.; Chien, H. C. R.; Hsu, W. H. Production of *N*-acetyl-d-neuraminic acid by recombinant whole cells expressing *Anabaena* sp. CH1 *N*-acetyl-d-glucosamine 2-epimerase and *Escherichia coli N*-acetyl-d-neuraminic acid lyase. *J. Biotechnol.* **2007**, *129*, 453−460.
(39) Zhu, D.; Zhan, X.; Wu, J.; Gao, M.; Zhao, Z. Efficient whole-cell biocatalyst for Neu5Ac production by manipulating synthetic, degradation and transmembrane pathways. *Biotechnol. Lett.* **2017**, *39*, 55−63.
(40) Uchida, Y.; Tsukada, Y.; Sugimori, T. Purification and properties of *N*-acetylneuraminate lyase from *Escherichia coli*. *J. Biochem.* **1984**, *96*, 507−522.
(41) Schnell, S. Validity of the Michaelis-Menten equation-steady-state or reactant stationary assumption: that is the question. *FEBS J.* **2014**, *281*, 464−472.
(42) Wu, Y.; Liu, J.; Han, X.; Meng, X.; Li, M.; Wang, J.; Xue, H.; Yang, Y.; Xu, P.; Tao, F. Eliminating host-guest incompatibility via enzyme mining enables the high-temperature production of *N*-acetylglucosamine. *iScience* **2023**, *26*, 105774.
(43) Jumper, J.; Evans, R.; Pritzel, A.; Green, T.; Figurnov, M.; Ronneberger, O.; Tunyasuvunakool, K.; Bates, R.; Žídek, A.; Potapenko, A.; Bridgland, A.; Meyer, C.; Kohl, S. A. A.; Ballard, A. J.; Cowie, A.; Romera-Paredes, B.; Nikolov, S.; Jain, R.; Adler, J.; Back, T.; Petersen, S.; Reiman, D.; Clancy, E.; Zielinski, M.; Steinegger, M.; Pacholska, M.; Berghammer, T.; Bodenstein, S.; Silver, D.; Vinyals, O.; Senior, A. W.; Kavukcuoglu, K.; Kohli, P.; Hassabis, D. Highly accurate protein structure prediction with AlphaFold. *Nature* **2021**, *596*, 583−589.
(44) Schymkowitz, J.; Borg, J.; Stricher, F.; Nys, R.; Rousseau, F.; Serrano, L. The FoldX web server: an online force field. *Nucleic Acids Res.* **2005**, *33*, W382−W388.

https://doi.org/10.1021/acs.jafc.3c07259
J. Agric. Food Chem. XXXX, XXX, XXX−XXX

(45) Zambrano, R.; Jamroz, M.; Szczasiuk, A.; Pujols, J.; Kmiecik, S.; Ventura, S. AGGRESCAN3D (A3D): server for prediction of aggregation properties of protein structures. *Nucleic Acids Res.* **2015**, *43*, W306−W313.
(46) Kumar, S.; Stecher, G.; Tamura, K. MEGA7: molecular evolutionary genetics analysis version 7.0 for bigger datasets. *Mol. Biol. Evol.* **2016**, *33*, 1870−1874.
(47) Zhang, H.; Gao, S.; Lercher, M. J.; Hu, S.; Chen, W. H. EvolView, an online tool for visualizing, annotating and managing phylogenetic trees. *Nucleic Acids Res.* **2012**, *40*, W569−W572.
(48) Irwin, J. J.; Shoichet, B. K. ZINC-a free database of commercially available compounds for virtual screening. *J. Chem. Inf. Model.* **2004**, *45*, 177−182.
(49) Zhao, H.; Caflisch, A. Discovery of ZAP70 inhibitors by high-throughput docking into a conformation of its kinase domain generated by molecular dynamics. *Med. Chem. Lett.* **2013**, *23*, 5721−5726.
(50) Abraham, M. J.; Murtola, T.; Schulz, R.; Páll, S.; Smith, J. C.; Hess, B.; Lindahl, E. GROMACS: High performance molecular simulations through multi-level parallelism from laptops to supercomputers. *SoftwareX* **2015**, *1−2*, 19−25.
(51) Mikulskis, P.; Genheden, S.; Ryde, U. Effect of explicit water molecules on ligand-binding affinities calculated with the MM/GBSA approach. *J. Mol. Model.* **2014**, *20*, 2273.
(52) Chen, X.; Zhou, J.; Zhang, L.; Pu, Z.; Liu, L.; Shen, W.; Fan, Y. Development of an *Escherichia coli*-based biocatalytic system for the efficient synthesis of *N*-acetyl-d-neuraminic acid. *Metab. Eng.* **2018**, *47*, 374−382.
(53) Arcus, V. L.; Mulholland, A. J. Temperature, dynamics, and enzyme-catalyzed reaction rates. *Annu. Rev. Biophys.* **2020**, *49*, 163−180.
(54) Fagerbakke, K. M.; Heldal, M.; Norland, S. Content of carbon, nitrogen, oxygen, sulfur and phosphorus in native aquatic and cultured bacteria. *Aquat. Microb. Ecol.* **1996**, *10*, 15−27.
(55) Tsuchido, T.; Katsui, N.; Takeuchi, A.; Takano, M.; Shibasaki, I. Destruction of the outer-membrane permeability barrier of *Escherichia-coli* by heat-treatment. *Appl. Environ. Microbiol.* **1985**, *50*, 298−303.
(56) Guo, M.; Zhang, L.; He, Q.; Arabi, S. A.; Zhao, H.; Chen, W.; Ye, X.; Liu, D. Synergistic antibacterial effects of ultrasound and thyme essential oils nanoemulsion against *Escherichia coli* O157:H7. *Ultrason. Sonochem.* **2020**, *66*, 104988.
(57) Park, S.; Kazlauskas, R. J. Biocatalysis in ionic liquids - advantages beyond green technology. *Curr. Opin. Biotechnol.* **2003**, *14*, 432−437.
(58) Peleg, M. Temperature-viscosity models reassessed. *Crit. Rev. Food Sci. Nutr.* **2018**, *58*, 2663−2672.
(59) Chang, R. L.; Andrews, K.; Kim, D.; Li, Z.; Godzik, A.; Palsson, B. O. Structural systems biology evaluation of metabolic thermotolerance in *Escherichia coli*. *Science* **2013**, *340*, 1220−1223.

https://doi.org/10.1021/acs.jafc.3c07259
J. Agric. Food Chem. XXXX, XXX, XXX−XXX